Exhaust Plume Structure in a Quasi-Steady MPD Accelerator

ADAM P. BRUCKNER* AND ROBERT G. JAHN†
Princeton University, Princeton, N.J.

Spectroscopic and photographic investigations reveal a complex azimuthal species structure in the exhaust plume of a quasi-steady argon MPD accelerator. Over a wide range of operating conditions the injected argon remains collimated in discrete jets which are azimuthally in line with the six propellent injector orifices. The regions between these argon jets, including the core of the exhaust flow, are occupied by impurities such as carbon, hydrogen, and oxygen ablated from the Plexiglas insulator plate in the arc chamber. Time-resolved spectroscopic velocity measurements, obtained by a scanning Fabry-Perot spectrometer system at a current of 16 ka and a mass flow of 6 g/sec, indicate an argon ion jet velocity of 1.7×10^4 m/sec, which considerably exceeds the Alfvén critical speed. It is found that half the observed final velocity is attained in an acceleration region well downstream of the region of significant electromagnetic interaction. Temperature measurements indicate that simple gasdynamic expansion processes in the argon jets can only partially explain this acceleration. Although there is evidence of some recombination from ionized states of the propellent, the energy recovered as directed motion is too small to be responsible for the high observed velocity. A transfer of momentum from the core flow of ablation products may contribute to the acceleration of the argon.

I. Introduction

QUASI-STEADY plasma accelerators have considerable potential as thrusters for deep space missions and have consequently been the subject of substantial research in recent years.[1-8] Much has been learned about the complex physical phenomena occurring in this class of thrusters, but there remain as yet many subtle processes which are only poorly understood. One of these is the exact nature of the acceleration mechanism. Much effort has been applied to unravel this problem, in particular through measurements of exhaust velocity patterns.[2,4,7-9] However, results published to date have not been in agreement. Using a cumbersome spectroscopic technique in two separate studies on a coaxial argon-fed MPD arc device similar to the one investigated here, Malliaris et al. have reported conflicting results.[7,8] In the first work argon exhaust velocities of 1.8×10^4 m/sec were measured, while in the more recent studies they found a limiting exhaust velocity equal to the so-called Alfvén critical speed—8.7×10^3 m/sec for argon—which has been proposed by some as a fundamental limit for MPD accelerators.[7-9] Jahn and Clark,[2] using electrostatic time of flight probes, have observed exhaust velocities of the order of 2.5×10^4 m/sec, which substantially exceeds both the Alfvén critical speed of argon and that computed from the electromagnetic thrust relation.[10] It is the primary task of the work described in this paper to resolve the controversy surrounding the exhaust velocity of argon-fed quasi-steady accelerators by carrying out a series of new velocity measurements.

The pure streaming velocity components in the MPD exhaust can be measured directly by means of spectroscopic Doppler-shift methods. Accordingly, a scanning Fabry-Perot interferometer system has been developed, which can record spectral line shifts and widths on a time scale more than an order of magnitude shorter than the length of the discharge current pulse.[11] Although this system permits time-resolved measurements of both velocity and temperature, without disturbing the exhaust flow or being subject to wave propagation effects, it is unable to provide local measurements. However, if the exhaust plume being studied is azimuthally uniform, local values of velocity and temperature can be obtained by the application of suitable Abel inversion procedures.[12]

Previous diagnostic measurements of magnetic fields,[1] potential profiles,[3,5] and impact pressure profiles[6] in the accelerator studied here indicated a complete cylindrical symmetry of these parameters, and consequently it had normally been assumed that the discharge luminosity patterns are azimuthally uniform also.[13] However, early experiments with the Fabry-Perot interferometer suggested otherwise,[14] indicating the existence of a complex but regular azimuthal and radial structure in the distribution of the argon propellent in the exhaust. The implications of this unexpected plume structure to the interpretation of Doppler-shift data led to an investigation of its nature and origins.[11,15] This study is summarized in Sec. III. The experimental measurement of velocity and temperature profiles of singly ionized argon, the dominant propellent specie in the exhaust, is then discussed in Sec. IV. Possible acceleration mechanisms are considered in the final portion of this paper.

II. MPD Arc Facility

The experiments described in this paper were performed in the accelerator shown schematically in Fig. 1. Briefly, the apparatus consists of a cylindrical discharge chamber of 12.5 cm diam, with a 1.9-cm-diam × 2.1 cm long conical tungsten cathode and an aluminum anode with a 10-cm-diam exhaust orifice, driven by a 3300 μfd × 8 kv matched capacitor line which can be arranged to deliver a variety of rectangular, nonreversing current pulses ranging from 4–26 ka × 1 msec to 16–100 ka × 250 μsec. Argon propellent gas is fed into the arc chamber through six injectors in the insulating Plexiglas end plate by means of a fast-acting solenoid valve. The mass flow is controlled by a calibrated orifice in the valve and by the propellent reservoir pressure. Another valve provides a gas pulse to the gas-triggered switch through a tube whose length is adjusted to synchronize switch breakdown with the achievement of steady cold gas flow in the accelerator chamber. Some 30 μsec after discharge initiation, the current and magnetic field distributions achieve a steady state which is maintained until the current ceases.[1]

Presented in part as Paper 72-499 at the AIAA 9th Electric Propulsion Conference, Bethesda, Md., April 17–19, 1972; submitted December 26, 1973. This work supported by NASA Grant NGL 31-001-005.

Index categories: Plasma Dynamics and MHD; Electric and Advanced Space Propulsion; Atomic, Molecular, and Plasma Properties.

* Graduate Student, Guggenheim Aerospace Propulsion Laboratories; presently Research Associate, Aerospace Research Laboratory, University of Washington, Seattle, Wash. Associate Member AIAA.

† Dean, School of Engineering and Applied Science. Associate Fellow AIAA.

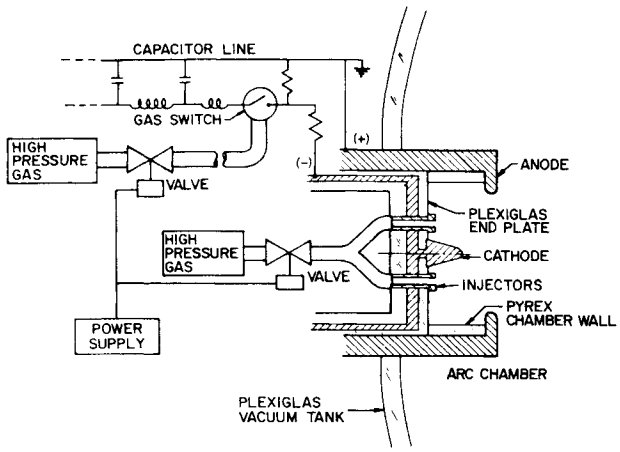

Fig. 1 Accelerator schematic.

III. Species Structure of the Exhaust

Considerable information on the structure of MPD arcs can be obtained from simple spectroscopic and visual observations.[11,13] Spectrograms have identified the various molecular, atomic, and ionic species participating in the discharge, and have provided clues to the structure of the exhaust. Spectra have been obtained at several locations in the arc chamber and exhaust plume, and the following radiating species have been identified: AI, AII, AIII, C_2, CII, CIII, HI, NII, OII, and WI, of which AII is the dominant specie. All of these constituents are contained in the propellent or materials of which the discharge chamber is constructed. Ideally, only the argon spectrum should be visible. The observation of many lines of carbon, hydrogen, oxygen, and nitrogen indicates that significant amounts of material from the Plexiglas and nylon components of the arc chamber are being ingested by the discharge. Of particular significance is the apparent concentration of ablation products near the centerline of the exhaust.

These spectroscopic studies have led to a simple method of determining the species distribution in the exhaust, namely the photography of the entire discharge through narrow-band spectral filters selected to isolate certain lines or groups of lines of the various radiating species.[11] By using a number of different lines of sight it has been possible to discover the three-dimensional distribution of each radiating constituent. Because of the quasi-steady nature of the discharge over most of the current pulse the photographs were recorded by simply opening the camera shutter for the duration of the current pulse. Both color slides and black and white prints were obtained in this manner.

With each filter used in these studies the discharge was photographed along five different lines of sight at the nominal operating condition of 16 ka × 1 msec at 6 g/sec argon flow. Two views through an interference filter of 10 Å bandwidth, which transmits the prominent 4879.9Å line of AII, are shown

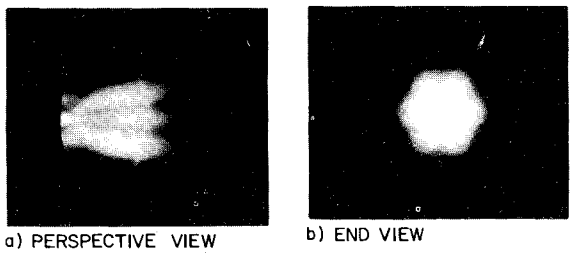

Fig. 2 Discharge at 4880 Å, showing distribution of AII. J = 16 ka $\dot{m}$ = 6 g/sec.

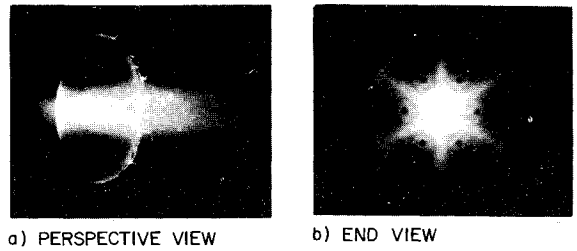

Fig. 3 Discharge at 5910 Å, showing distribution of CII and C_2. J = 16 ka, $\dot{m}$ = 6 g/sec.

in Fig. 2. The distribution of singly ionized argon exhibits a complex six-jet azimuthal structure related to the location of the mass injectors (which can be seen faintly in the end view). The argon jets maintain their identity at least three anode orifice diameters downstream of the anode face. (This is not evident in the reproductions in this paper, but is clearly visible in the original negatives.) Not surprisingly, photographs at other AII wavelengths reveal an identical luminous structure. By observing the shock wave patterns generated around a spherical glass probe positioned in and between the luminous argon jets it is deduced that streamlines of argon flow lie parallel to these luminous jets and that there is very little argon in the spaces between them.[11,15] This observation is corroborated by photographs of the exhaust plume obtained at other lines of sight, and by additional spectroscopic studies in the near ultraviolet and infrared.[11,14,16,17]

From the preceding it can be deduced that the regions devoid of argon must be occupied by the ablated impurities. This is indeed the case. Figure 3 displays two views of the discharge through a 5910 Å interference filter of 75 Å bandwidth, which transmits the 5889.97 Å and 5891.65 Å lines of CII, and the tail of the C_2 Swan band system whose head is at 6191.2 Å. The concentration of luminosity near the centerline of the exhaust is clearly visible. Figure 3b provides an end-on view of the azimuthal structure of the carbon impurities, indicating that it is the ablation pattern at the Plexiglas back plate of the arc chamber that leads to the complex species structure in the exhaust. Molecular carbon (C_2) is confined within the arc chamber and is found predominantly in the bright luminous star-shaped region (Fig. 3b) which extends about a cathode length from the Plexiglas base plate. There is no C_2 in the exhaust plume downstream of the cathode tip. The prominent axial jet seen to issue from the chamber in Fig. 3a consists of singly ionized carbon, CII. This specie is also found in the luminous star above the base plate, but occupies primarily the annular space between the cathode and the six injectors. The distribution of CII in the exhaust plume has itself a star-shaped cross section similar to the luminosity at the base plate. It fills the core of the flow and the gaps between the argon jets.

With the aid of spectroscopic data and other photographs through various spectral filters and at different viewing angles, it is determined that the other heavy impurity species, OII and NII, have the same concentration profiles as CII, and that hydrogen is found throughout the entire exhaust plume, even to some extent within the argon jets.

Operation at Other Conditions

In an effort to determine the effect of arc current and mass flow on the exhaust plume structure, a series of photographic experiments such as described previously was carried out at currents from 4 to 32 ka and argon mass flows of 3–12 g/sec. Interesting effects were observed and are discussed elsewhere.[11,15] In general, the exhaust exhibited varying degrees of species separation at all but highly overfed conditions. The structure was most sharply defined at the so-called "matched" operating conditions.

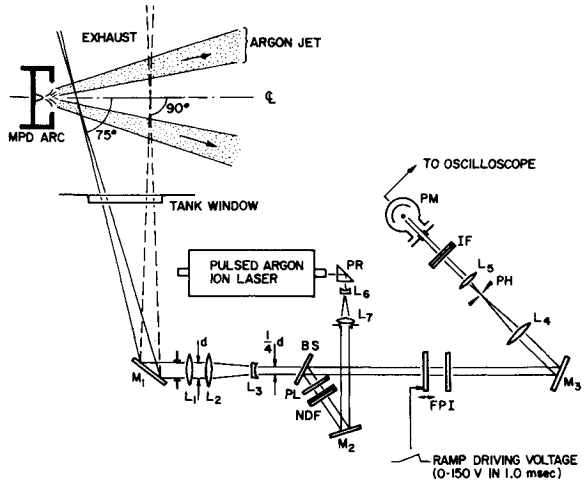

Fig. 4 Fabry-Perot interferometer system.

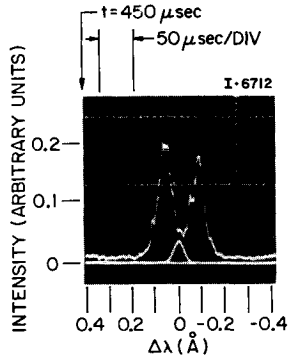

Fig. 5 Typical 4880 Å line profile at 10.9 cm from the anode exit plane. $J = 16$ ka, $\dot{m} = 6$ g/sec.

Ablation Phenomena

As has been already noted, the unusual species structure of the MPD exhaust is a result of the ablation of the Plexiglas insulator plate in the arc chamber. This ablation takes about 150 μsec to become fully developed, so that during the early stages of the arc discharge the exhaust does not exhibit a species inhomogeneity. The exact ablation mechanism remains uncertain but there is evidence that radiation and conduction effects are equally important. Recent investigations have demonstrated that the mass injection geometry has a strong influence on the insulator erosion. A search for the optimum geometry to minimize ablation is in progress. Also being investigated are various refractory materials which have better ablation resistance than Plexiglas.[17]

IV. Velocity and Temperature Measurements

The discovery of the complex species structure in the exhaust of the MPD arc requires a reinterpretation of the time-of-flight velocity data of Ref. 2. In particular, the reported centerline exhaust velocities of 2.5×10^4 m/sec are seen to correspond to the velocity of the light ablation products, rather than of the heavier argon propellent as was earlier believed. The spectroscopic Doppler-shift technique described below can easily measure the pure streaming velocity of the argon, but the lack of cylindrical symmetry in its distribution in the flow precludes the reduction of the data to purely local values by the standard Abel inversion techniques. Nevertheless, the rather well-defined collimation of the argon jets does allow a deduction of average velocity and temperature as functions of axial distance within the individual argon jets.

Experimental Apparatus

The high spectral resolution (~0.05 Å) necessary to detect velocities of the order of 10^4 m/sec and temperatures of the order of 1 ev is easily achieved with a Fabry-Perot interferometer.[11,18-20] The instrument used in the present investigation is capable of scanning operation by means of a piezoelectric translator, at a sweep rate of about 0.003 Å/μsec, with an over-all finesse of about 25. The interferometer and its supporting optics are shown schematically in Fig. 4. Light from the discharge is directed by mirror M_1 to the objective lens L_1, whose focal point lies on the discharge axis. The mirror can be adjusted about both horizontal and vertical axes to obtain the desired line of sight through the exhaust plume. Lenses L_2 and L_3 reduce the beam diameter by a factor of four, so that only the central portion of the Fabry-Perot plates is used. Mirror M_3 directs the interferometer output to the lens L_4 which focuses the center of the scanning fringe pattern on a 0.8-mm-diam pinhole, PH. Lens L_5 collimates the light from the pinhole for passage through a 10 Å bandwidth interference filter, IF, which selects the 4879.9 Å line of AII. An RCA 1P28 photomultiplier tube detects the scanned fringes. A TRW pulsed argon ion laser provides the reference wavelength at 4879.9 Å against which Doppler shifts are measured. Its output is expanded by lens system L_6-L_7 and superimposed on the discharge light by means of mirror M_2 and a clear glass beam splitter, BS. A set of polarizers, PL, and neutral density filters, NDF, is used to control the laser intensity. The entire system is enclosed in a sound absorbing metal box atop a heavy optical table which is vibration isolated from the floor of the laboratory. All measurements carried out with this system were confined to the nominal arc operating condition of $J = 16$ ka, $\dot{m} = 6$ g/sec.

Surveys at 90° Lines of Sight

Extensive radial surveys were carried out at four axial positions, 4.6, 10.9, 15.9, and 30.6 cm from the anode exit plane, with the lines of sight perpendicular to the discharge axis. A typical spectral line profile obtained with the line of sight passing through two diametrically opposed argon jets, 10.9 cm from the anode, is shown in Fig. 5. The trace is the scan of the 4879.9 Å spectral line of AII by the interferometer system at a time about 600 μsec into the discharge current pulse. The spectral line exhibits a characteristic Doppler split which results from the opposed radial velocity components of the two argon jets intersected by the line of sight. The small trace under the central minimum corresponds to the reference wavelength of 4879.9 Å provided by the laser.

Measurements of line intensity off-axis, both above and below the centerline at the four axial positions investigated have identified the loci of maximum jet luminosity. These loci turn out to be straight lines inclined at 15° to the axis and are reasonable first approximations to the average flow direction in each argon jet.

Surveys at 75° Lines of Sight

Another series of Doppler-shift velocity measurements was made at five additional axial stations with the lines of sight at

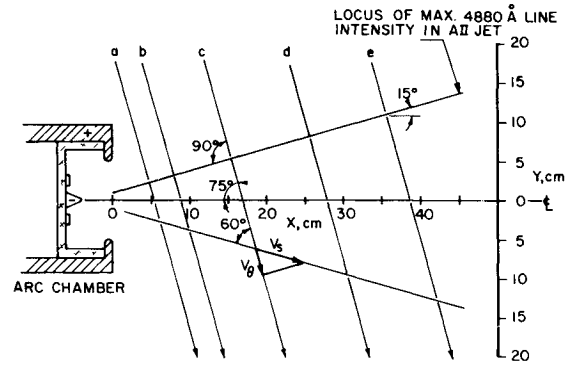

Fig. 6 Lines of sight used in 75° velocity measurements.

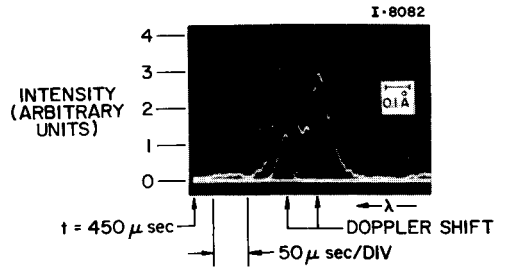

Fig. 7 Profile and Doppler-shift of 4880 Å AII line on line of sight crossing axis at 75° at 16.8 cm from the anode exit plane. $J = 16$ ka, $\dot{m} = 6$ g/sec.

an angle of 75° to the discharge axis, passing through two diametrically opposed jets (Fig. 6). These lines of sight are thus approximately perpendicular to one of the jets and make about a 60° angle with the other. The observed split line profile should therefore consist of a shifted and an unshifted component. This is evident in Fig. 7, obtained with a line of sight crossing the axis 16.8 cm from the anode face. The "unshifted," more intense peak on the left corresponds to the far jet, intersected at ~ 90° while the smaller, blue-shifted peak on the right corresponds to the near jet intersected at ~ 60° The small line profile under the "unshifted" peak is the laser reference wavelength, recorded immediately prior to firing the arc. The absolute Doppler-shift between the laser reference and the near jet is somewhat less than that between the two jets, indicating that the true "average" velocity vector of the argon in the jets makes an angle somewhat greater than 15° with the axis.

Once the velocity components at 75° and at 90° to the axis are known as functions of axial position along the argon jets, both the magnitude and direction of the average velocity vector in the jets as functions of axial distance can be easily calculated. The axial variation of velocity along each argon jet is shown in Fig. 8. The velocity increases from 8.5×10^3 m/sec at $x = 5$ cm to ~ 1.7×10^4 m/sec at $x = 40$ cm, where x is the distance measured from the arc chamber exit plane. The bulk of the acceleration occurs within a distance of about 15 cm. The average jet flow angle increases from ~ 17° at 5 cm to ~ 20° at 18 cm and remains constant at ~ 20° thereafter.

It is interesting to note that while at $x = 5$ cm the velocity is virtually equal to the Alfvén critical speed of argon, the final velocity attained is very nearly twice this value. In effect then, the Alfvén critical speed does not impose a fundamental limitation on the attainable exhaust velocity.

Using measured values of magnetic field strength, total particle density, temperature, and flow velocity at $x = 5$ cm it can be shown that the magnetic pressure is nearly three orders of magnitude smaller than the gas pressure, which in turn is about

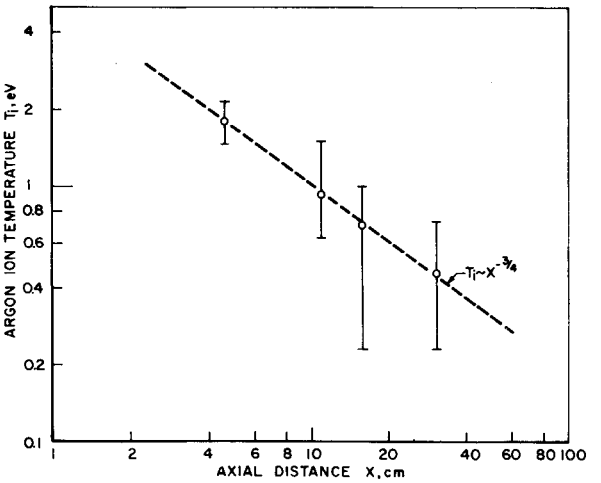

Fig. 9 Development of ion temperature in argon jets.

one order of magnitude smaller than the dynamic pressure.[11] It can thus be safely assumed that $x = 5$ cm defines the downstream limit of the electromagnetic acceleration region. Consequently, the acceleration downstream of this location, from 8.5×10^3 m/sec to the final value of 1.7×10^4 m/sec, is not of electromagnetic origin. The concept of the Alfvén critical speed thus cannot be applied to the entire exhaust flow of the thruster. The concept has validity only when applied to that region of the exhaust where electromagnetic effects dominate, namely upstream of $x = 5$ cm in the present case. The picture that emerges, then, is one of two distinctly different acceleration regions—the first of predominantly electromagnetic origin, which brings the injected propellent up to the Alfvén critical speed, and the second, as yet unspecified, which subsequently accelerates the gas to a velocity much higher than the Alfvén speed. It has been suggested that the high final velocity could be a result of significant conversion of thermal energy to directed kinetic energy in the flow.[4] To test this hypothesis it is necessary to examine axial temperature profiles of heavy particles and electrons.

Temperature Measurements

Argon ion temperatures in the jets have been determined from measurements of widths of the line profiles obtained in the 90° line of sight surveys. Suitable corrections have been made for instrumental broadening and the broadening due to radial velocity dispersion in the jets. Other broadening mechanisms, such as the Stark and Zeeman effects and microturbulence, are not significant under the conditions existing in the exhaust plume. Figure 9 shows the development of average argon ion tempera-

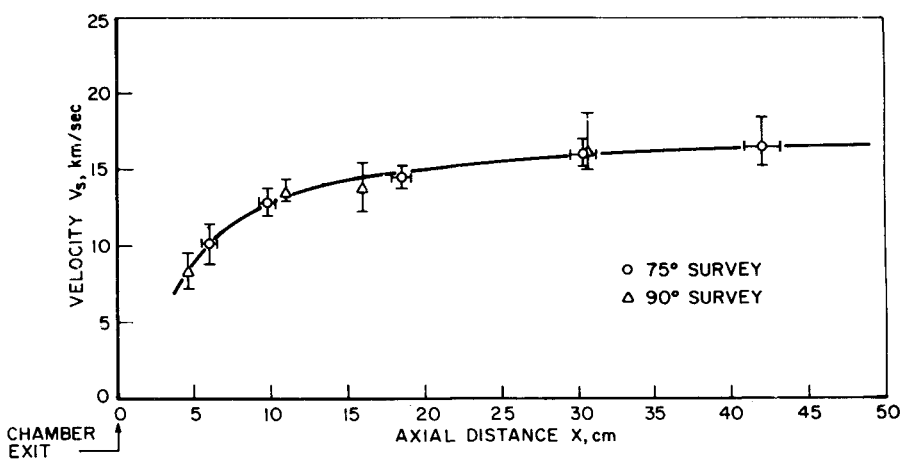

Fig. 8 Development of argon ion jet velocity.

ture in the jets. The temperature profile can be approximated by an inverse power law, $T_i \sim x^{-3/4}$, where x is the distance from the anode exit plane. It decreases from ~ 1.8 ev at $x = 5$ cm to ~ 0.5 ev at $x = 30$ cm. Electron temperature data in the exhaust are as yet sparse, however, twin Langmuir probe measurements in and near the chamber,[3] and recent double floating probe investigations at $x = 25$ cm in the argon jets[21] indicate that the electron temperature decreases from about 1.7 ev at $x = 5$ cm to about 0.8 ev at $x = 25$ cm, following approximately a power law of the form $T_e \sim x^{-1/2}$.

Possible Acceleration Mechanisms of Nonelectromagnetic Origin

Calculations based on these temperature data indicate that if electrothermal conversion is to explain the acceleration beyond $x = 5$ cm in the plume, almost all the static flow enthalpy available at $x = 5$ cm, including ionization and excitation energy, would have to be recovered as directed kinetic energy. Available evidence does not justify this conclusion. Besides the fact that the ion and electron temperatures are not in equilibrium, evidence of substantial recombination of AII to AI between $x = 5$ cm and $x = 20$ cm, the axial interval where the bulk of the acceleration occurs, is ambiguous. The neutral specie has been observed spectroscopically throughout the exhaust, but primarily at the outskirts of the plume and far downstream beyond $x = 36$ cm, where the exhaust velocity has essentially attained a constant value.[17] Since the observed spectra are not time-resolved, it is not certain that the AI radiation near the exhaust orifice is produced exclusively during the driving current pulse. There is independent evidence of considerable afterglow radiation,[22] thus the AI spectrum could in part be produced after cessation of the current pulse. Alternatively, the AI spectrum could be a result of some propellent bypassing the discharge region. A definitive evaluation of the recombination of AII must await more detailed time-resolved spectroscopy.

Spectral lines of the doubly ionized specie, AIII, have been found in the arc chamber and in the argon jets within about 5 cm from the anode exit.[16] Experimental evidence of some recombination of this specie exists. Assuming three-body recombination is dominant[23] and using a simple quasi-one-dimensional flow model, it can be shown that less than 10% of this AIII could recombine to AII by $x = 20$ cm, under the prevailing flow conditions. Even if all the ionization energy that is released were recovered as streaming energy it would contribute only a very small fraction ($< 3\%$) of the observed velocity increment. As it is, with the temperatures and densities found in the exhaust, more than half the available recombination energy would be lost as radiation from cascading and resonance transitions which follow electron capture in the three-body process. Although AI radiation has been observed in the exhaust, the recombination of AII to AI has not been identified as a significant contributor to the acceleration in the region between $x = 5$ cm and $x = 20$ cm. The only remaining energy substantially available for recovery as streaming motion thus would be that of the random thermal motion of the ions and electrons which, even if complete, would contribute only about one-third of the observed velocity increment downstream of $x = 5$ cm.

The dominant acceleration mechanism downstream of $x = 5$ cm thus remains uncertain. Undoubtedly, electrothermal conversion and recombination play partial roles, as suggested previously. One mechanism not yet discussed is a possible transfer of momentum from the core flow of ablation products to the argon jets. Existing measurements of centerline velocity profiles show that the core flow attains much higher velocities than the argon in the jets, namely $\sim 2.5 \times 10^4$ m/sec,[2] probably as a result of the lower molecular weight of the ablation products. Furthermore, axial profiles of centerline velocity exhibit a relative minimum in precisely that interval where the argon in the jets undergoes the bulk of its acceleration, a result which is consistent with a momentum transfer model. Because of the complexity of the flow geometry resulting from the species inhomogeneity, and the difficulties associated with freely expanding flows of high enthalpy plasmas, no attempt has been made to examine the momentum transfer hypothesis of argon acceleration analytically. This mechanism must therefore also remain purely conjectural until the problem of insulator ablation is eliminated. Velocity measurements on an uncontaminated argon exhaust should resolve the extent to which the presently observed argon velocity profile is due to interaction with the flow of ablation products.

V. Conclusions

The physical picture which emerges from the experiments reported here is that the exhaust plume of the quasi-steady MPD arc is considerably more complicated than heretofore believed. The exhaust plume exhibits a complex species structure related to the position of the propellent injectors and to the ablation pattern on the arc chamber insulator. This observation partially explains the discrepancy in velocity measurements carried out by different researchers. Previously measured centerline velocities of 2.5×10^4 m/sec on the device investigated here[2] are now seen to have corresponded to the central core flow of ablated products rather than to the argon propellent. The work of Malliaris et al.[7,8] is more difficult to put in perspective because it is not known to what extent insulator ablation occurred in their experiments. The measurements of argon exhaust velocity described here have revealed that it attains a value of 1.7×10^4 m/sec, considerably exceeding the Alfvén critical speed. This result agrees closely with the early results of Malliaris[7] but not with his subsequent work.[8] The indications are that there exist two regions in the exhaust where distinctly different acceleration processes are at work. In the first region, which encompasses the interior of the arc chamber and the part of the exhaust flow within half an anode orifice diameter of the chamber exit, the dominant mechanism is of electromagnetic origin, accelerating the propellent to the Alfvén critical speed. The other region includes the remainder of the exhaust plume downstream of the region of significant electromagnetic interaction. In this outer region the flow accelerates to a velocity nearly twice the Alfvén critical speed. The exact mechanism is not yet fully understood. Recombination from the ionized states of argon does not appear to be an adequate acceleration mechanism and recovery of random thermal energy also only partially accounts for the observed velocity increment. It is possible that a momentum transfer from the high-speed core flow of light ablation products to the argon jets may contribute to the acceleration of the argon. In any case, the Alfvén critical velocity appears not to impose a fundamental limitation on the attainable exhaust velocity.

References

[1] Clark, K. E. and Jahn, R. G., "Quasi-Steady Plasma Acceleration," *AIAA Journal*, Vol. 8, No. 2, Feb. 1970, pp. 216–220.

[2] Jahn, R. G. et al., "Acceleration Patterns in Quasi-Steady MPD Arcs," *AIAA Journal*, Vol. 9, No. 1, Jan. 1971, pp. 167–172.

[3] Turchi, P. J. and Jahn, R. G., "Cathode Region of a Quasi-Steady MPD Arc Jet," *AIAA Journal*, Vol. 9, No. 7, July 1971, pp. 1372–1379.

[4] Di Capua, M. S., "Energy Deposition in Parallel-Plate Plasma Accelerators," Ph.D. thesis, Aerospace and Mechanical Sciences Rept. 1015, Dec. 1971, Princeton University, Princeton, N.J.

[5] Oberth, R. C. and Jahn, R. G., "Anode Phenomena in High Current Accelerators," *AIAA Journal*, Vol. 10, No. 1, Jan. 1972, pp. 86–91.

[6] Clark, K. E., Jahn, R. G., and von Jaskowsky, W. F., "Distribution of Momentum and Propellant in a Quasi-steady MPD Discharge," AIAA Paper 72-497, Bethesda, Md., 1972.

[7] Malliaris, A. C. and John, R. R., "Outstanding Problems Regarding the Feasibility of a Repetitively Pulsed MPD Propulsion System," AIAA Paper 70-1093, Stanford, Calif., 1970.

[8] Malliaris, A. C. et al., "Quasi-Steady MPD Propulsion at High Power," Final TR AVSD-0146-71-RR, CR111872, Feb. 1971, NASA.

[9] Nerheim, N. M. and Kelly, A. J., "A Critical Review of the Magnetoplasmadynamic (MPD) Thruster for Space Applications," NASA TR 32-1196, Feb. 1968, Jet Propulsion Lab., Pasadena, Calif.

[10] Jahn, R. G., *Physics of Electric Propulsion*, McGraw-Hill, New York, 1968.

[11] Bruckner, A. P., "Spectroscopic Studies of the Exhaust Plume of

a Quasi-Steady MPD Accelerator," Ph.D. thesis, Aerospace and Mechanical Sciences Rept. 1041, May 1972, Princeton University, Princeton, N.J.

[12] Bohn, W. L. et al., "On Spectroscopic Measurements of Velocity Profiles and Non-Equilibrium Radial Temperatures in an Argon Plasma Jet," *Journal of Quantitive Spectroscopy and Radiative Transfer*, Vol. 7, 1967, pp. 661–676.

[13] Clark, K. E. et al., "Quasi-Steady Magnetoplasmadynamic Arc Characteristics," AIAA Paper 70-1095, Stanford, Calif., 1970.

[14] Jahn, R. G. et al., "Pulsed Electromagnetic Gas Acceleration," NASA NGL 31-001-005, Aerospace and Mechanical Sciences Rept. 634q, July 1971, Princeton University, Princeton, N.J.

[15] Bruckner, A. P. and Jahn, R. G., "Exhaust Plume Structure in a Quasi-Steady MPD Arc," AIAA Paper 72-499, Bethesda, Md., 1972.

[16] Jahn, R. G. et al., "Pulsed Electromagnetic Gas Acceleration," NASA NGL 31-001-005, Aerospace and Mechanical Sciences Rept. 634s, July 1972, Princeton University, Princeton, N.J.

[17] Jahn, R. G. et al., "Pulsed Electromagnetic Gas Acceleration," NASA NGL 31-001-005, Aerospace and Mechanical Sciences Rept. 634t, Jan. 1973, Princeton University, Princeton, N.J.

[18] Meissner, K. W., "Interference Spectroscopy," *Journal of the Optical Society of America*, Vol. 31, No. 6, June 1941, pp. 405–427.

[19] Jacquinot, P., "New Developments in Interference Spectroscopy," *Reports on Progress in Physics*, Vol. XXII, 1960, pp. 267–312.

[20] Greig, J. R. and Cooper, J., "Rapid Scanning with the Fabry-Perot Etalon," *Applied Optics*, Vol. 7, No. 11, Nov. 1968, pp. 2166–2170.

[21] Jahn, R. G. et al., "Pulsed Electromagnetic Gas Acceleration," NGL 31-001-005, Aerospace and Mechanical Sciences Rept. 634r, Jan. 1972, Princeton University, Princeton, N.J.

[22] von Jaskowsky, W. F., private communication, 1973, Dept. of Aerospace and Mechanical Sciences, Princeton University, Princeton, N.J.

[23] Zel'dovich, Ya. B. and Raizer, Yu. P., *Physics of Shock Waves and High Temperature Hydrodynamic Phenomena*, Academic Press, New York, 1966, Vol. 1, pp. 406–413 and Vol. 2, pp. 571–585.

AIAA JOURNAL VOL. 12, NO. 9

Jet-Diagnostics of a Self-Field Accelerator with Langmuir Probes

F. MAISENHÄLDER* AND W. MAYERHOFER†
DFVLR-Institut für Plasmadynamik, Stuttgart, F. R., Germany

Cylindrical electric probes of the Langmuir type are used to investigate the jet of a self-field plasma accelerator. The test conditions with argon as propellant range from $I = 2000$ amp to 4500 amp and $\dot{m} = 0.3$ g/sec to 1.0 g/sec. The pattern of the flow direction, the radial and axial distributions of the electron temperature, the ion density, the static pressure, the ratio of directed to thermal velocity, and the ion velocity are determined. The electron temperature profiles show steep gradients from the axis of the jet to a radius of about 8 cm. Beyond this radius the temperatures remain at a nearly constant value of $8-10\times10^3$K in the whole visible region of the jet with a diameter of about 1 m. The influence of the angle of attack on the determination of the electron temperature turns out to be not severe. The ion densities, calculated from the ion saturation currents and the electron temperatures, are affected by the discharge currents and the mass flow rates. In the axis peak values are observed up to 5×10^{14} cm^{-3}. An increase of the mass flow rate causes large radial density gradients over a wide range of the diameter. The calculated distributions of the static pressure show that "entrainment" can be excluded. This is confirmed by the flow pattern of the ions and the total gas too. The ratios of V/V_{th} (a quantity which may be regarded as a Mach number) are in good agreement with calculated Mach numbers. The profiles of the ion velocity show a reasonable behavior. The mass flow through a cross section of the jet calculated from the velocity and density profiles is in good agreement with the applied mass flow rate. Observations of characteristic parameters show that in a wide region of the plasma the probes are operated collision free, but that in the axis near the nozzle exit a transition regime to collision-dominated conditions is present.

Introduction

THE plasma accelerator of the self-magnetic or self-field coaxial type may be operated continuously or pulsed. The pulsed quasi-steady version[1–5] probably will find its main application as a thruster. The continuously working accelerator designed for purposes of propulsion too, will have its near future application as a wind-tunnel device. Theoretical and experimental investigations of this accelerator have been done by Hügel.[6,7] For reasons of completeness a short description of the mechanism of this type of accelerator will be given here.

The thruster consists of a cathode made of thoriated tungsten, an arc chamber, and an expansion nozzle. Arc chamber and nozzle are made of individual water-cooled segments which are insulated against each other by layers of alumina (Fig. 1). The propellant is fed along the cathode. The last and largest of the segments represents the anode. The outer surface of the accelerator, with exception of the anode front face, is insulated by a layer of alumina too, thus achieving a well defined onset of the discharge current. Two mechanisms contribute to the plasma acceleration: 1) electrothermal heating of the plasma and expansion in the nozzle, and 2) acting of $\mathbf{j}\times\mathbf{B}$ volume forces

Presented as Paper 73-1095 at the AIAA 10th Electric Propulsion Conference, Lake Tahoe, Nev., October 31–November 2, 1973; submitted November 26, 1973; revision received March 25, 1974. The authors wish to thank Th. Peters who sponsored this work. Furthermore we would like to acknowledge the assistance of F. Albrecht and R. Jacobson in constructing the test facilities and of M. Kling in establishing the programs for the evaluation of the data.

Index categories: Plasma Dynamics and MHD; Electric and Advanced Space Propulsion.

* Senior Research Scientist.

† Research Scientist.